

Levels in ^{99}Pd populated by the $^{96}\text{Ru}(\alpha, n)$ and $^{6}\text{Li}, p2n$ reactions

J. Dubuc, G. Kajrys, P. Larivière, N. Nadon, S. Pilotte, and S. Monaro
Laboratoire de Physique Nucléaire, Université de Montréal, Montréal, Québec, Canada H3C 3J7

J. C. Waddington

Nuclear Physics Laboratory, University of McMaster, Hamilton, Ontario, Canada L3S 4K1

(Received 22 September 1987)

The structure of ^{99}Pd has been investigated via the $^{96}\text{Ru}(\alpha, n)$ and $^{96}\text{Ru}({}^6\text{Li}, p2n)$ reactions in an attempt to populate low- and high-spin levels of this nucleus. Excitation functions and angular distributions of deexcitation γ rays have been measured to determine the spins of the levels deduced in γ - γ coincidence measurements carried out at 18 MeV (α particles) and 38 MeV (${}^6\text{Li}$ particles), respectively. Several new excited levels are found in the present measurements and the results show that the level structure of ^{99}Pd bears a strong resemblance to that of the isotone ^{97}Ru . It appears also that ^{99}Pd may fit nicely into the systematics evinced in the heavier odd- A Pd nuclei.

I. INTRODUCTION

Strongly populated cascades of stretched $E2$ transitions have been found in the odd- A palladium and ruthenium isotopes.¹⁻⁶ These cascades appear to be built on relatively pure single-particle states such as $d_{5/2}$, $g_{7/2}$, and $h_{11/2}$ and can be interpreted as decoupled bands. The existence of these bands may be indicative that the odd- A Ru and Pd isotopes are weakly deformed rotational nuclei and thus can be described by a particle-rotor model. Indeed, this picture seems to be valid for the neutron-rich isotopes of this region^{7,8} but it appears less applicable to the neutron-deficient nuclei ^{95}Ru and ^{97}Ru .^{6,9} Evidently the approaching of the magic neutron number $N=50$ enhances the shell effects in these nuclei making their excitation modes more complex. The ^{99}Pd ($N=53$) nucleus should provide an unusual opportunity of observing the effects due to the presence of few neutrons above the closed $N=50$ shell. Prior to the present work the excited states of ^{99}Pd have not been investigated very extensively. An initial study via (HI, xn) experiments¹⁰ seemed to indicate that the structure of this nucleus had very little in common with that observed in $^{101,103,105}\text{Pd}$.¹⁻³ However, subsequent work¹¹⁻¹³ showed that a large part of the structure evinced in ^{99}Pd could only be assigned to ^{99}Rh and that only the band built on the $g_{7/2}$ state at 264 KeV could be considered as belonging to ^{99}Pd .

The low-spin states of ^{99}Pd following the EC- β^+ decay of ^{99}Ag have been studied by Huyse *et al.*¹⁴ who suggested the spins of some low-lying levels. In this work we wish to present the results of an investigation of the low- and high-spin states in ^{99}Pd populated via the $^{96}\text{Ru}(\alpha, n)$ and $^{96}\text{Ru}({}^6\text{Li}, p2n)$ reactions, respectively.

II. EXPERIMENTAL PROCEDURE

The in-beam γ -ray spectroscopy measurements on ^{99}Pd were performed at two different accelerators. The first experiment was done at the University of Montréal EN

Tandem accelerator where low- and medium-spin states of ^{99}Pd were populated via the $^{96}\text{Ru}(\alpha, n)$ reaction using a ^{96}Ru target (98% enriched and ~ 10 mg/cm² thick) sintered on a thick tantalum backing. Excitation functions were measured at 12, 15, 16, 17, and 18 MeV bombarding energy using a Ge(Li) counter having a resolution of 2.1 keV at 1.33 MeV and placed at 15 cm from the target at 45° to the beam direction. The same detector was employed to carry out the angular distribution measurements at 18 MeV bombarding energy. The detector was placed at 25 cm from the target and positioned successively at 15° intervals between 0° and 90° to the beam direction. A current integrator together with another Ge(Li) detector placed at -90° to the beam direction served as normalization monitors. γ - γ coincidence measurements were performed using two Ge(Li) detectors having a resolution of about 2 keV and placed at 90° and -55° to the beam direction. Standard timing techniques were employed with a time resolution of ~ 15 ns. The coincidence data were event-mode recorded onto magnetic tapes for subsequent playback and analysis.

The second experiment was performed at the University of McMaster FN Tandem accelerator where medium- and high-spin states of ^{99}Pd were populated via the $^{96}\text{Ru}({}^6\text{Li}, p2n)$ reaction using the same target described above. An array of 5 HPGe detectors and 6 NaI counters were used to collect the γ - γ coincidence information which was obtained at a beam energy of 38 MeV. The 5 HPGe detectors were placed in a horizontal plane at 5°, 22°, 45°, 67°, and 100° to the beam direction, whereas the NaI counters were located at the back, below, and above the diffusion chamber and were used as γ -ray multiplicity filters. The accepted events, which consisted of at least 3 Ge detectors or 2 Ge detectors and 1 NaI firing, were recorded onto magnetic tapes and constructed into a 4096×4096 channel coincidence matrix. From this matrix, one-dimensional spectra for any gated γ -ray energy could be subsequently extracted. An angular distribution experiment was also carried out at 38 MeV bombarding energy using the 5 HPGe detectors gat-

ed by the six-element NaI multiplicity filter. The requirement here was to have 1 Ge detector and 1 NaI counter firing. Furthermore, yields of γ rays were also measured at 30, 35, and 38 MeV bombarding energy employing the Ge detector placed at 100° to the beam direction in a singles mode. The angular distribution and excitation function spectra from both reactions were analyzed with the peak fitting code SAMPO (Ref. 15) while the procedures given by Taras and Haas¹⁶ were employed in the analysis of the angular distribution data. As an illustration of our data, Fig. 1 shows a typical γ -ray singles spectrum while some examples of relative yields of deexcitation γ rays and γ - γ coincidence spectra are shown in Figs. 2, 3, and 4, respectively.

III. RESULTS

The level scheme of ^{99}Pd as deduced in this work is shown in Fig. 5, while a summary of level energies, γ -ray energies, and angular distribution results is presented in Table I.

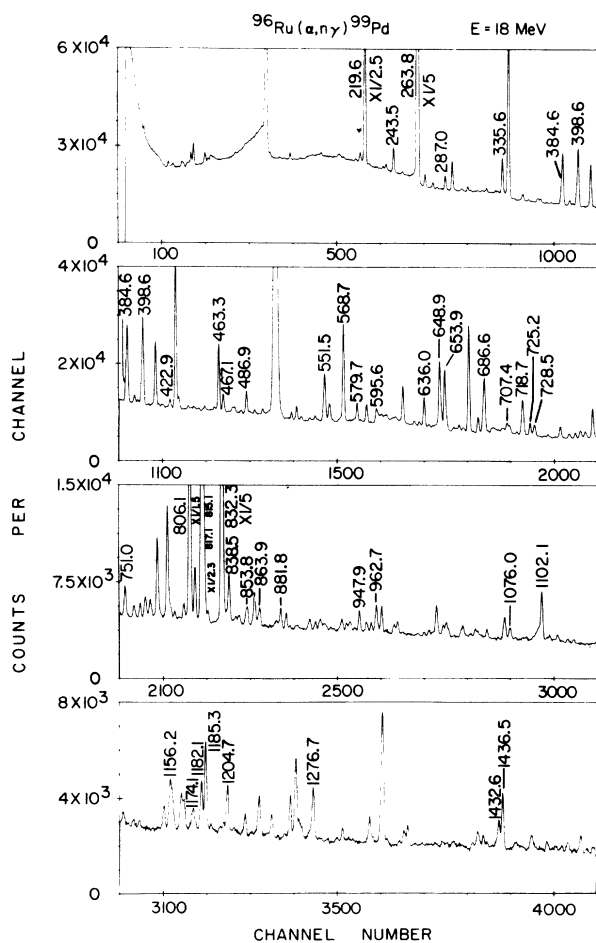


FIG. 1. A typical spectrum from the $^{96}\text{Ru}(\alpha, n)$ reaction taken at $E_\alpha = 18$ MeV. Energies are in keV and labeled peaks belong to ^{99}Pd unless otherwise indicated.

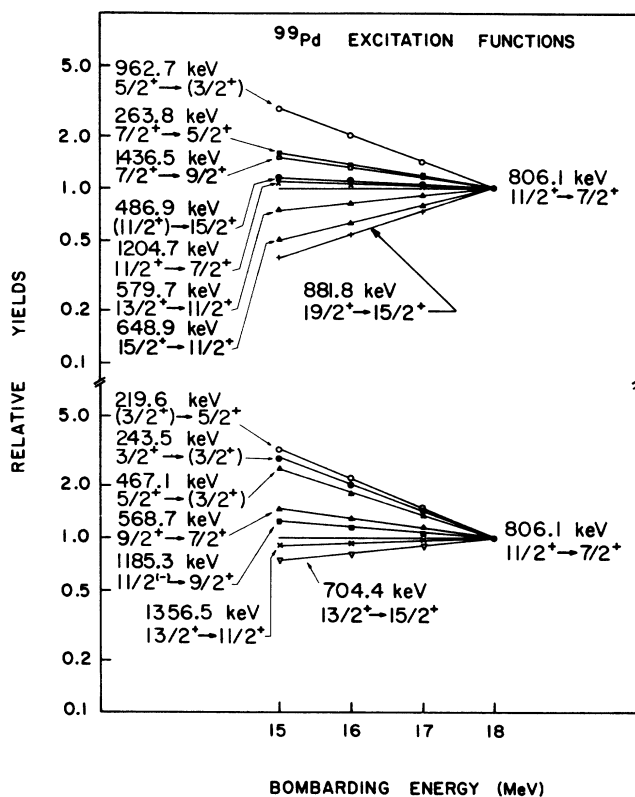


FIG. 2. Relative excitation functions of selected γ -ray transitions in ^{99}Pd from the reaction $^{96}\text{Ru}(\alpha, n)$. The yields are normalized to that of the 806.1 ($\frac{11}{2}^+ \rightarrow \frac{7}{2}^+$) keV transition.

A. The 0.0, 219.6, and 263.8 keV levels

No direct measurements on the spin-parity of the ground state of ^{99}Pd exist. However, the characteristics of the ^{99}Pd ground state decay make a $\frac{5}{2}^+$ spin assignment very plausible, and this value is adopted here since it is also expected from valid systematic considerations in this nuclear region and agrees well with a plethora of data on transitions decaying to it. The 219.6 keV level was detected in the disintegration of ^{99}Ag by Huyse *et al.*¹⁴ who suggested a spin of $\frac{3}{2}^+$. Our excitation func-

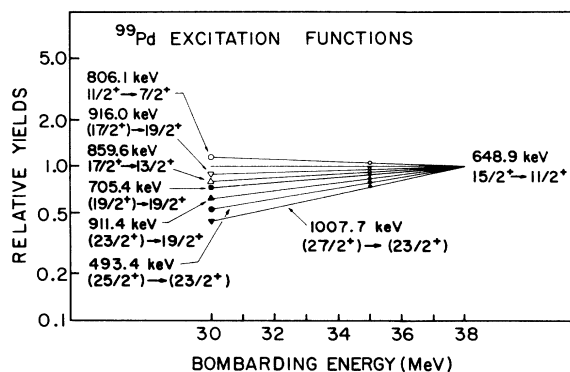


FIG. 3. Relative excitation functions of selected γ -ray transitions in ^{99}Pd from the reaction $^{96}\text{Ru}({}^6\text{Li}, p2n)$. The yields are normalized to that of the 648.9 ($\frac{15}{2}^+ \rightarrow \frac{11}{2}^+$) keV transition.

TABLE I. A summary of level energies, γ -ray energies, relative intensities, and angular distribution results obtained in this work for ^{99}Pd .

E_x (keV)	E_γ (keV)	Relative ^a intensity (%)	$J_i^\pi \rightarrow J_f^\pi$	A_2^a	A_4^a	δ^b
0.0			$\frac{5}{2}^+$			
219.6	219.6	86.9(40)	$(\frac{3}{2}^+) \rightarrow \frac{5}{2}^+$	-0.076(60)	0.060(70)	
263.8	263.8 ^c		$\frac{7}{2}^+ \rightarrow \frac{5}{2}^+$			
463.3	243.5	9.5(9)	$\frac{3}{2}^+ \rightarrow (\frac{3}{2}^+)$			
	463.3	40.6(25)	$\rightarrow \frac{5}{2}^+$	-0.015(30)	-0.025(45)	
555.2	335.6	13.0(11)	$(\frac{5}{2}, \frac{7}{2}) \rightarrow (\frac{3}{2}^+)$			
686.6	422.9	3.5(5)	$\frac{5}{2}^+ \rightarrow \frac{7}{2}^+$			
	467.1	10.1(10)	$\rightarrow (\frac{3}{2}^+)$	0.146(65)	-0.034(75)	
	686.6	65.0(45)	$\rightarrow \frac{5}{2}^+$	0.445(45)	-0.130(55)	1.2 \pm 0.4
815.3	551.5 ^c		$\frac{7}{2}^+ \rightarrow \frac{7}{2}^+$			
	595.6 ^c		$\rightarrow (\frac{3}{2}^+)$			
	815.3	116.0(70)	$\rightarrow \frac{5}{2}^+$	-0.525(45)	0.078(55)	1.4 \pm 0.4
832.5	568.7	75.1(55)	$\frac{9}{2}^+ \rightarrow \frac{7}{2}^+$	0.360(30)	0.115(40)	-1.1 \pm 0.5
	832.5 ^c		$\rightarrow \frac{5}{2}^+$			
1069.9	806.1	100.0	$\frac{11}{2}^+ \rightarrow \frac{7}{2}^+$	0.355(35)	-0.080(45)	<i>E2</i>
1102.3	287.0	6.1(6)	$\frac{9}{2}^+ \rightarrow \frac{7}{2}^+$	-0.250(50)	0.050(60)	<i>M1</i>
	838.5	28.1(20)	$\rightarrow \frac{7}{2}^+$	0.608(50)	0.225(60)	-1.9 $^{+1.0}_{-3.9}$
	1102.3	37.4(25)	$\rightarrow \frac{5}{2}^+$	0.310(35)	-0.060(45)	<i>E2</i>
1182.2	962.7	14.4(9)	$\frac{5}{2}^+ \rightarrow (\frac{3}{2}^+)$	-0.330(40)	-0.015(5)	-0.13 \pm 0.07
	1182.1	9.5(9)	$\rightarrow \frac{5}{2}^+$	0.158(35)	-0.035(45)	
1419.8	1156.0 ^c		$\rightarrow \frac{7}{2}^+$			
1468.5	398.6 ^c		$\frac{11}{2}^+ \rightarrow \frac{11}{2}^+$			
	636.0	20.6(12)	$\rightarrow \frac{9}{2}^+$	-0.725(40)	0.035(50)	0.7 $^{+0.8}_{-0.6}$
	653.2 ^c		$\rightarrow \frac{7}{2}^+$			
	1204.7	23.2(9)	$\rightarrow \frac{7}{2}^+$	0.325(35)	-0.060(45)	<i>E2</i>
1540.5	725.2(10)	13.2(10)	$\frac{9}{2}^+ \rightarrow \frac{7}{2}^+$	-0.260(40)	0.045(50)	<i>M1</i>
	853.8	15.1(18)	$\rightarrow \frac{5}{2}^+$	0.284(35)	-0.068(45)	<i>E2</i>
	1276.7	21.8(9)	$\rightarrow \frac{7}{2}^+$	0.150(75)	0.110(85)	
1649.5	579.7	10.2(8)	$\frac{13}{2}^+ \rightarrow \frac{11}{2}^+$	-0.788(55)	0.080(65)	0.8 $^{+0.3}_{-1.0}$
	817.0	96.3(60)	$\rightarrow \frac{9}{2}^+$	0.260(35)	-0.060(45)	<i>E2</i>
1696.4	863.9	9.6(8)	$\frac{9}{2}^+ \rightarrow \frac{9}{2}^+$	0.135(40)	-0.020(50)	
	1432.6	13.2(10)	$\rightarrow \frac{7}{2}^+$	-0.248(60)	-0.065(70)	
1718.8	648.9	83.5(35)	$\frac{15}{2}^+ \rightarrow \frac{11}{2}^+$	0.410(40)	-0.115(50)	<i>E2</i>
1853.3	384.6 ^c		$\frac{9}{2}^+ \rightarrow \frac{11}{2}^+$			
	751.0	17.5(8)	$\rightarrow \frac{9}{2}^+$	0.425(45)	-0.125(55)	-0.8 \pm 0.2
2006.6	1174.1	5.7(7)	$(\frac{7}{2}, \frac{9}{2}) \rightarrow \frac{9}{2}^+$	0.520(40)	-0.095(50)	
2017.8	947.9	14.5(9)	$\frac{11}{2}^{(-)} \rightarrow \frac{11}{2}^+$	0.307(37)	-0.018(45)	
	1185.3	32.9(14)	$\rightarrow \frac{9}{2}^+$	-0.165(35)	0.040(45)	
2062.5	1230.0		$\rightarrow \frac{9}{2}^+$			
2145.7	1076.0	8.2(9)	$\frac{11}{2} \rightarrow \frac{11}{2}^+$	0.564(60)	-0.140(70)	-0.5 \pm 1.0
2205.7	486.9	12.3(8)	$(\frac{11}{2}^+) \rightarrow \frac{15}{2}^+$	0.290(40)	-0.060(50)	<i>E2</i>
2269.0	728.5	11.8(9)	$\frac{7}{2}^+ \rightarrow \frac{9}{2}^+$	-0.315(40)	-0.030(50)	
	1436.5	26.1(20)	$\rightarrow \frac{9}{2}^+$	-0.265(45)	0.000(55)	
2426.0	707.4	11.6(10)	$\frac{13}{2}^+ \rightarrow \frac{15}{2}^+$	0.375(40)	0.010(50)	0.7 $^{+0.3}_{-1.3}$
	1356.5	9.5(15)	$\rightarrow \frac{11}{2}^+$	-0.205(40)	0.050(50)	
2437.3 ^d	718.7 ^c		$\rightarrow \frac{15}{2}^+$			
2481.6 ^d	832.0 ^c		$\rightarrow \frac{13}{2}^+$			
2508.9 ^d	859.6	88.8(98)	$\frac{17}{2}^+ \rightarrow \frac{13}{2}^+$	0.325(50)	-0.105(60)	<i>E2</i>
2600.6	881.8	13.1(9)	$\frac{19}{2}^+ \rightarrow \frac{15}{2}^+$	0.328(37)	-0.090(45)	<i>E2</i>
2740.0 ^d	1022.0 ^c		$\rightarrow \frac{15}{2}^+$			

TABLE I. (Continued).

E_x (keV)	E_γ (keV)	Relative ^a intensity (%)	$J_i^\pi \rightarrow J_f^\pi$	A_2^a	A_4^a	δ^b
3306.0 ^d	705.4	92.5(95)	$(\frac{19}{2}^+) \rightarrow \frac{19}{2}^+$	0.385(70)	-0.095(80)	
3512.0 ^d	911.4	100	$\frac{23}{2}^+ \rightarrow \frac{19}{2}^+$	0.410(50)	-0.110(60)	$E2$
3516.4 ^d	916.0	49.5(75)	$(\frac{17}{2}^+) \rightarrow \frac{19}{2}^+$			
3572.4 ^d	972.0 ^c		$\rightarrow \frac{19}{2}^+$			
4005.4 ^d	493.4	88.0(99)	$\frac{25}{2}^+ \rightarrow \frac{23}{2}^+$	-0.225(45)	0.005(55)	
4519.7 ^d	1007.7	17.8(25)	$\frac{27}{2}^+ \rightarrow \frac{23}{2}^+$	0.395(60)	-0.105(70)	$E2$

^aThe intensity values have been measured at an alpha beam energy of 18 MeV. Uncertainties in the least significant figures are indicated in parentheses.

^bRose and Brink convention (Ref. 17).

^cDoublet.

^dThe intensities of the γ rays deexciting these levels have been measured via the $^{96}\text{Ru}(^6\text{Li}, p2n)$ reaction at 38 MeV. The intensity values have been normalized to that of the 911.4 keV transition. The contribution coming from ^{99}Rh produced via the $^{96}\text{Ru}(^6\text{Li}, 2pn)$ reaction has been taken into account in determining the intensity values of the 493.4 and 859.6 keV γ rays.

tion data on the 219.6 keV transition supports a $\frac{3}{2}$ spin assignment which is consistent with its isotropic angular distribution.

The 263.8 keV γ -ray deexciting the 263.8 keV level is a composite transition (from the decay of ^{99}Pd to ^{99}Rh) thus its angular distribution and excitation function data are of limited use. The $\frac{7}{2}^+$ assignment is adopted here since it fits well with data on γ -rays populating this state and it is also strongly supported by systematic considerations. The ground and second excited states of ^{99}Pd have, most probably, a $2d_{5/2}$ and $1g_{7/2}$ configuration, respectively, whereas the $\frac{3}{2}^+$, 219.6 keV level, which seems to have very little interaction with the main structure of ^{99}Pd , has probably a more complex configuration in agreement with similar levels observed in many nuclei of this mass region.

B. The 463.3, 555.2, and 686.6 keV levels

The 463.3 and 686.6 keV levels were already observed in the decay of ^{99}Ag (Ref. 14) while the 555.2 keV state is new. The excitation function data on the 243.5 and 463.3 keV γ -rays deexciting the 463.3 keV state suggest a spin of $\frac{3}{2}$ which is consistent with the isotropic angular distribution of the 463.3 keV transition. The coincidence between the 335.6 keV transition and the 219.6 keV γ ray supports the existence of the 555.2 keV level on which very little can be said since the 335.6 keV γ ray is very weak even though its yield curve suggests a spin of $\frac{5}{2}$ or $\frac{7}{2}$. The excitation function data on the 467.1 and 686.6 keV γ rays deexciting the 686.6 keV level suggest a $\frac{5}{2}$ spin assignment to this state, which is supported by their angular distributions. A weak 422.9 keV transition de-

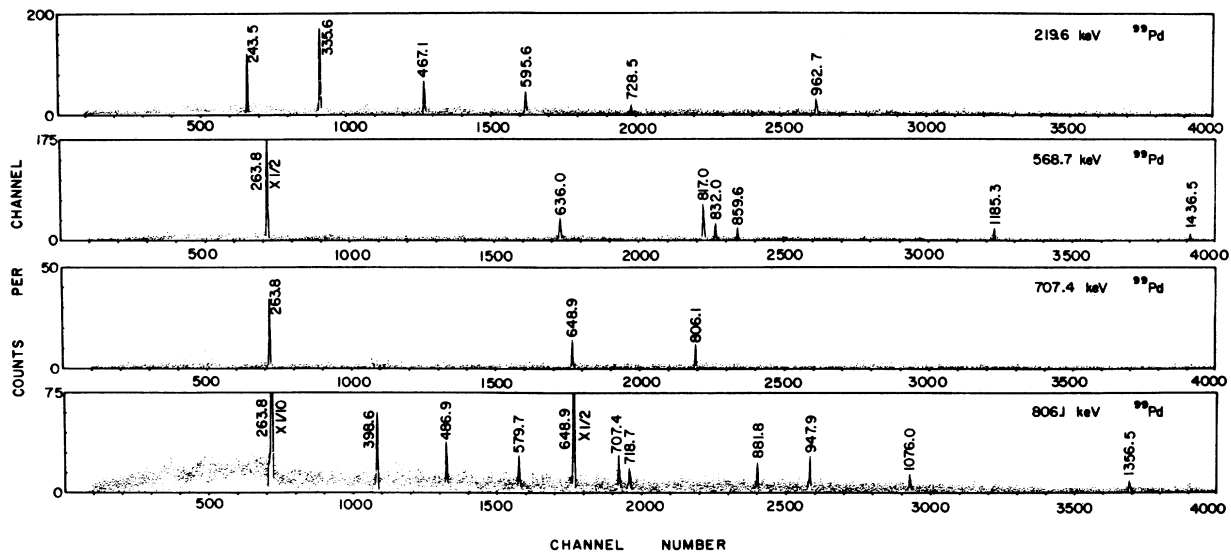


FIG. 4. Some examples of the γ - γ coincidence spectra obtained from the $^{96}\text{Ru}(\alpha, n)$ (219.6 and 806.1 keV gates) and $^{96}\text{Ru}(^6\text{Li}, p2n)$ reactions (568.7 and 707.4 keV gates).

caying to the 219.6 keV level seems present in the coincidence data. From the decay mode of this level a positive parity seems very probable.

C. The 815.3 and 832.5 keV levels

An intense 815.3 keV line in the singles and coincidence spectra confirm the existence of the 815.3 keV level already observed in decay work.¹⁴ A spin of $\frac{7}{2}$ is strongly favored from the excitation and angular distribution data on the 815.3 keV γ ray. Transitions of 551.5 and 595.6 keV also deexcite this level but very little information can be extracted from them since the former γ ray is a doublet and the latter is difficult to analyze being contaminated by the 596 keV transition coming from the (n,n' γ) reaction on ⁷⁴Ge. From the decay mode of the 815.3 keV state a positive parity is very probable.

The 832.5 keV state was already detected in the decay of ⁹⁹Ag (Ref. 14) and is confirmed in this work via coincidence data. A $\frac{9}{2}^+$ spin-parity assignment is strongly suggested by the excitation function and angular distribution data on the 568.7 keV transition populating the $\frac{7}{2}^+$, 263.8 keV state. No information can be extracted from the 832.5 keV γ ray, this transition being a doublet, a large fraction of which comes from the Coulomb excitation of the first excited state in ⁹⁶Ru.¹⁹ However, a $\frac{9}{2}^+$ assignment is indirectly suggested from data on γ rays populating this state. We cannot confirm the existence of a 816.1 keV level proposed by Huyse *et al.*¹⁴ since we have no evidence for this state.

D. The 1069.9, 1102.3, 1182.2, and 1419.8 keV levels

An intense transition of 806.1 keV deexcites the 1069.9 keV level. A spin of $\frac{11}{2}$ is strongly supported by the excitation function of the 806.1 keV γ ray which agrees with its characteristic $\Delta J=2$ angular distribution. The $\frac{11}{2}^+$ 1069.9 keV level belongs to the band built on the $g_{7/2}$ 263.8 keV state already observed in previous works,¹⁰⁻¹² and strongly excited up to the spin of $\frac{27}{2}^+$ in this study via the (⁶Li,p2n) reaction. The 1102.3 and 1182.2 keV levels were already observed in the decay of ⁹⁹Ag and a $\frac{7}{2}^+$ spin assignment was suggested for the 1182.2 keV state. However, our excitation function and angular distribution data support a $\frac{9}{2}^+$ assignment to the 1102.3 keV level and a $\frac{5}{2}^+$ for the 1182.2 keV state. The 1419.8 keV level is evinced via the (263.8–1156.0) keV weak coincidence. No spin assignment can be given on this state since the 1156.0 keV γ ray is a doublet. It should be mentioned that the same level was possibly detected in decay work¹⁴ but at 1423.5 keV.

E. The 1468.5, 1540.5, 1649.5, and 1696.4 keV levels

These levels were already observed in the decay of ⁹⁹Ag (Ref. 14) and only for the 1696.4 keV state a spin parity

of $\frac{7}{2}^+$ was proposed. The 1468.5 keV level is deexcited by the 398.6, 636.0, 653.2, and 1204.7 keV γ rays. The 398.6 and 653.2 keV transitions are doublets and no information could be extracted from them. However, the excitation functions and angular distributions of the other two γ rays strongly suggest a $\frac{11}{2}$ spin assignment to this level, whose parity is probably positive from its decay mode. Spin-parity assignments of $\frac{9}{2}^+$ and $\frac{13}{2}^+$ to the 1540.5 and 1649.5 keV levels, respectively, are suggested from our data. The 1649.5 keV state seems to belong to the $d_{5/2}$ band which is strongly excited in the present work via the (⁶Li,p2n) reaction.

Finally, a $\frac{9}{2}$ spin is assigned to the 1696.4 keV level in disagreement with the $\frac{7}{2}^+$ value proposed by Huyse *et al.*¹⁴ We have no evidence either in the singles spectra or in the coincidence data for the 1476.3 keV γ ray which those authors placed as decaying to the $\frac{3}{2}^+$, 219.6 keV level. The characteristic $\Delta J=0$ and $\Delta J=1$ angular distributions of the 863.9 and 1432.6 keV transitions, respectively (see Table I) strongly support the $\frac{9}{2}$ spin assignment to the 1696.4 keV state, whose parity should be positive from its decay mode.

F. The 1718.8, 1853.3, and 2006.6 keV levels

An intense transition of 648.9 keV deexcites the 1718.8 keV level. A spin of $\frac{15}{2}$ is strongly supported from its excitation function which is consistent with its $\Delta J=2$ characteristic angular distribution. The $\frac{15}{2}^+$, 1718.8 keV level belongs to the strong cascade built on the $g_{7/2}$ 263.8 keV state in agreement with previous studies.¹⁰⁻¹² The 1853.3 and 2006.6 keV levels are weakly excited in the present work. However, a spin of $\frac{7}{2}$ is strongly supported by the excitation function of the 751.0 keV γ ray deexciting the 1853.3 keV level which is consistent with its $\Delta J=0$ characteristic angular distribution. No information on the 1853.3 keV level can be extracted from the 384.6 keV γ ray populating the $\frac{11}{2}^+$, 1468.5 keV state since this transition is a doublet in the singles spectrum. The data on the weak 1174.1 keV γ ray deexciting the 2006.6 keV state to the $\frac{9}{2}^+$, 1102.3 keV level supports a $\frac{9}{2}$ spin assignment to the former level even though a spin value of $\frac{7}{2}$ cannot be discarded from its excitation function.

G. The 2017.8, 2062.5, and 2145.7 keV levels

The first two levels are proposed here for the first time while the third level seems to have been excited also in the ⁹⁹Ag decay.¹⁴ The (1185.3–832.5) and (947.9–806.1–263.8) keV coincidences suggest the existence of the 2017.8 keV level while the 2062.5 and 2145.7 keV states are based exclusively on the (1230.0–832.5) and (1076.0–806.1–263.8) keV coincidences, respectively. However, since the former coincidence is detected only in the (⁶Li,p2n) reaction and no results can be extracted from

the angular distribution and excitation function data on the 1230.0 keV transition, we leave the 2062.5 keV level as dotted in the decay scheme. The other two states are detected more strongly in the (α, n) reaction and the exci-

tation function and angular distribution data on the γ rays deexciting them suggest spin assignments of $\frac{11}{2}$. Either one of these two states could be the $h_{11/2}$ level expected at about 2 Mev in ^{99}Pd as shown in Fig. 6 where

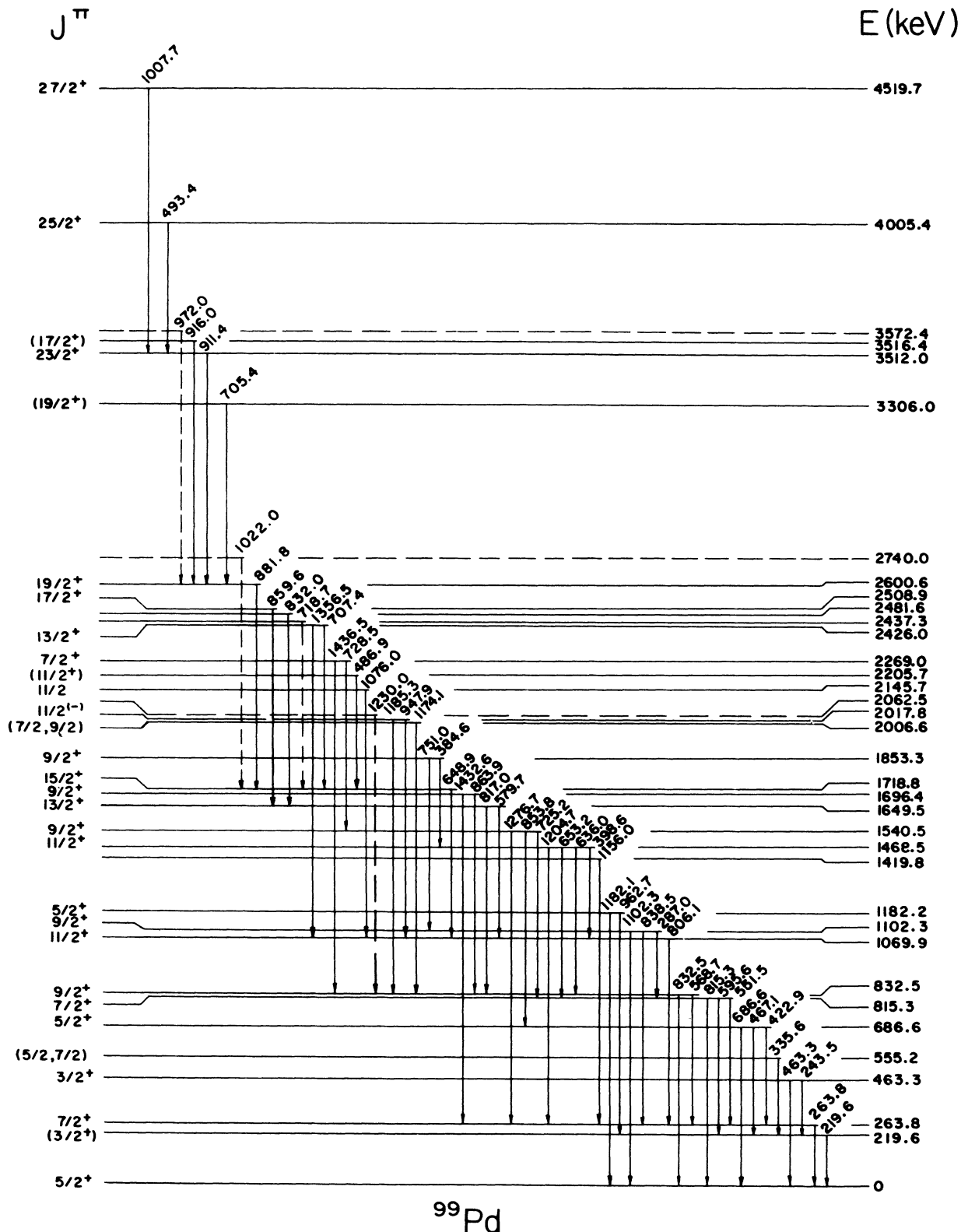


FIG. 5. The level scheme of ^{99}Pd . Energies are in keV. Dotted transitions and levels are considered probable but not definitively established.

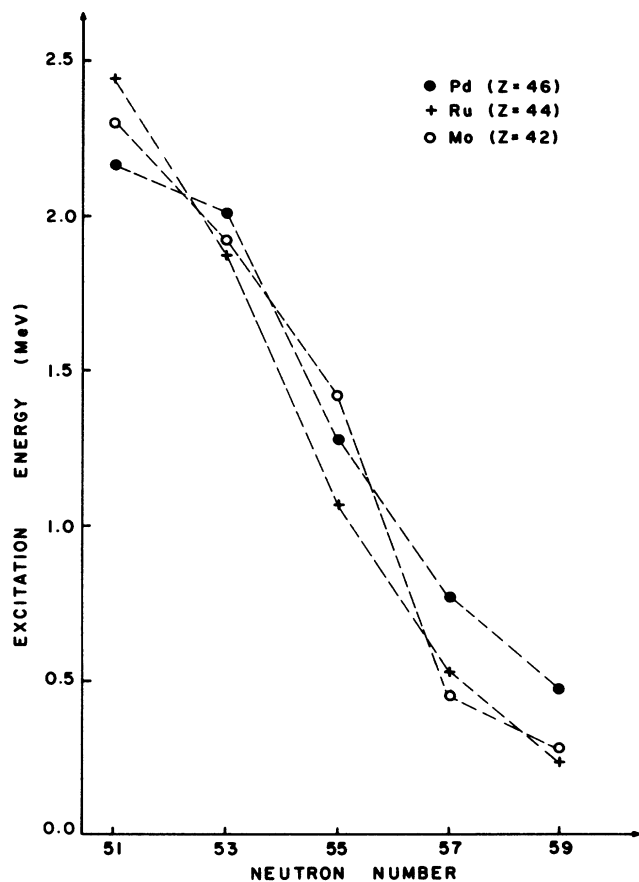


FIG. 6. The $\frac{1}{2}^-$ bandhead energies for odd- A Mo, Ru, and Pd nuclei plotted as a function of the neutron number N . The data on the Mo isotopes have been taken from Ref. 18. The data on the Ru isotopes have been taken from Refs. 4–6 and the data from the Pd isotopes have been taken from Refs. 1–3 and 20 (^{97}Pd).

the known $\frac{1}{2}^-$ bandhead energies in the odd- A Pd, Ru, and Mo isotones are plotted as a function of the neutron number N .

The 2017.8 keV level has been chosen in Fig. 6 as the more probable $\frac{1}{2}^-$ state in ^{99}Pd since its decay characteristics are very similar to those displayed by the same levels in the ^{95}Mo (Ref. 18) and ^{97}Ru (Refs. 6 and 9) isotones and in ^{101}Pd (Ref. 1) and ^{103}Pd .² Clearly the $h_{11/2}$ state is weakly excited in ^{99}Pd and no band built on it has been observed, whereas $\frac{15}{2}^- \rightarrow \frac{11}{2}^-$ transitions have been detected in ^{95}Mo (Ref. 18) and ^{97}Ru .^{6,9}

H. The 2205.7, 2269.0, and 2426.0 keV levels

All these levels have been established via both the (α, n) and $(^6\text{Li}, p2n)$ reaction. The data on the 486.9 keV transition deexciting the 2205.7 keV state would support a $\frac{1}{2}^+$ spin-parity assignment while the data on the 707.4 and

1356.5 keV γ rays deexciting the 2426.0 keV level suggest a $\frac{13}{2}^+$ spin-parity assignment. The 2269.0 keV level is inferred by the (1436.5-832.5) and (728.5-1276.7) keV coincidences. The angular distribution and excitation function data on the 728.5 and 1436.5 keV transitions support a $J = \frac{7}{2}$ spin assignment to the 2269.0 keV level whose parity is probably positive from its decay mode.

I. The 2437.3, 2481.6, 2508.9, and 2600.6 keV levels

A 718.7 keV transition is seen in coincidence with the (648.9-806.1-263.8) keV cascade establishing a level at 2437.3 keV. However, the 718.7 keV γ ray is an unresolved doublet in the singles spectrum and no information can be extracted from it. For the same reason no spin-parity assignment can be given for the 2481.6 keV level deexcited by a 832.0 keV transition (see 832.5 keV state). The 2508.9 keV level, which is essentially excited in the $(^6\text{Li}, p2n)$ reaction, is based exclusively on the (859.6-817.0) and (859.6-579.7) keV coincidences with the 817.0 and 579.7 keV γ rays deexciting the $\frac{13}{2}^+$ 1649.5 keV state. The excitation function and angular distribution data on the 859.6 keV transition support a $\frac{17}{2}^+$ spin-parity assignment to the 2508.9 keV level which is probably the $\frac{17}{2}^+$ member of the band built on the $d_{5/2}$ ground state. The 2600.6 keV level is deexcited by an intense 881.8 keV transition whose characteristics strongly suggest a spin of $\frac{19}{2}^+$ for the 2600.6 keV state in agreement with previous studies.¹⁰⁻¹²

J. The 2740.0, 3306.0, 3512.0, 3516.4, 3572.4, 4005.4, and 4519.7 keV levels

All these levels are established only via the $(^6\text{Li}, p2n)$ reaction. The levels at 2740.0 and 3572.4 keV are left as dotted in the decay scheme (see Fig. 4) since these two states are determined only by weak coincidences, and the 1022.0 and 972.0 keV transitions deexciting them are unresolved doublets in the singles spectrum. The 3306.0, 3512.0, and 3516.4 keV levels are proposed via coincidence measurements since the 705.4, 911.4, and 916.0 keV γ rays deexciting them are seen in coincidence with the transitions belonging to the band built on the 263.8 keV $g_{7/2}$ state. The excitation function and angular distribution data on the 705.4, 911.4, and 916.0 keV transitions suggest spins of $\frac{19}{2}$, $\frac{23}{2}$, and $\frac{17}{2}$, respectively, with probable positive parity. The $\frac{23}{2}^+$ spin-parity assignment to the 3512.0 keV level is in agreement with previous studies.^{10,11} Relatively intense lines of 493.4 and 1007.7 keV are seen in coincidence with the γ rays which deexcite the levels belonging to the $g_{7/2}$ band. From our data, spin parity of $\frac{25}{2}^+$ and $\frac{27}{2}^+$ are suggested for the 4005.4 and 4519.7 keV levels, respectively. The existence of the former level was also established by Piel and Scharff-Goldhaber¹¹ who, however, did not propose any spin assignment.

IV. DISCUSSION

A spectroscopy study of ^{99}Pd has been made via the $^{96}\text{Ru}(\alpha, n)$ and $^{96}\text{Ru}(^6\text{Li}, p2n)$ reactions to improve the knowledge of its level structure. The most important finding of the present work is the assessment in this nucleus of yrast cascades built on the $d_{5/2}$ and $g_{7/2}$ ground and second excited state, respectively. The finding of the high-spin cascade built on the 263.8 keV $\frac{7}{2}^+$ level definitely confirms its existence¹⁰⁻¹² while the other yrast cascade is reported here for the first time. Moreover, "unfavored," or less aligned states, which probably belong to either cascade, have also been detected together with many more levels whose origin is less clear. Similar positive-parity bands together with a negative-parity band built on the $h_{11/2}$ state have been also found in

many other nuclei around the $A=100$ region,¹⁻⁶ and their existence has been well explained in terms of a slightly modified rotation-aligned coupling model.^{7,8} The same picture, however, should be taken with caution in the case of ^{99}Pd since its level structure could be explained also by the quasiparticle phonon-coupling model. Such a possibility was already considered for the ^{97}Ru isotone whose structure bears an amazing resemblance with that of ^{99}Pd (Refs. 6 and 9) (see below). In fact, since specific theoretical calculations on ^{99}Pd are practically nonexistent, it would be worthwhile to compare the present results with those found in the isotone ^{97}Ru and also in the adjacent odd- A Pd nuclei with particular emphasis on ^{101}Pd . If one considers the palladium isotopes starting from ^{105}Pd (Refs. 1-3) to ^{99}Pd , it is immediately clear that the band built on the $g_{7/2}$ state is more and

TABLE II. Partial comparison of the decay properties of low lying levels in ^{97}Ru , ^{99}Pd , and ^{101}Pd .

E_x (keV)	E_γ (keV)	$J_i^\pi \rightarrow J_f^\pi$	δ	Isotope ^a
1199.3	320.2	$\frac{11}{2}^+(g_{7/2}) \rightarrow \frac{9}{2}^+(d_{5/2})$	$2.3^{+0.8}_{-0.5}$	97
	777.6	$\rightarrow \frac{7}{2}^+(g_{7/2})$	$E2$	97
1069.9	NF ^b	$\frac{11}{2}^+(g_{7/2}) \rightarrow \frac{9}{2}^+(d_{5/2})$		97
	806.1	$\rightarrow \frac{7}{2}^+(g_{7/2})$	$E2$	99
938.9	271.4	$\frac{11}{2}^+(g_{7/2}) \rightarrow \frac{9}{2}^+(d_{5/2})$	$0.05 \leq \leq 0.13$	101
	678.8	$\rightarrow \frac{7}{2}^+(g_{7/2})$	$E2$	101
1229.6	350.5	$\frac{9}{2}^+(g_{7/2}) \rightarrow \frac{9}{2}^+(d_{5/2})$		97
	389.4	$\rightarrow \frac{7}{2}^+(d_{5/2})$	$M1$	97
	807.9	$\rightarrow \frac{7}{2}^+(g_{7/2})$	$-3.1^{+4.8}_{-1.3}$	97
	1229.6	$\rightarrow \frac{5}{2}^+(d_{5/2})$	$E2$	97
1102.3	NF ^b	$\frac{9}{2}^+(g_{7/2}) \rightarrow \frac{9}{2}^+(d_{5/2})$		99
	287.0	$\rightarrow \frac{7}{2}^+(d_{5/2})$	$M1$	99
	838.5	$\rightarrow \frac{7}{2}^+(g_{7/2})$	$-1.9^{+1.0}_{-3.9}$	99
	1102.3	$\rightarrow \frac{5}{2}^+(d_{5/2})$	$E2$	99
1199.3	531.8	$\frac{9}{2}^+(g_{7/2}) \rightarrow \frac{9}{2}^+(d_{5/2})$		101
	611.3	$\rightarrow \frac{7}{2}^+(d_{5/2})$		101
	938.6	$\rightarrow \frac{7}{2}^+(g_{7/2})$		101
	1199.3	$\rightarrow \frac{5}{2}^+(d_{5/2})$	$E2$	101
2020.3	400.4	$\frac{13}{2}^+(g_{7/2}) \rightarrow \frac{11}{2}^+(d_{5/2})$		97
	821.0 ^c	$\rightarrow \frac{11}{2}^+(g_{7/2})$		97
NF ^b		$\frac{13}{2}^+(g_{7/2})$		99
	2041.9	$\frac{13}{2}^+(g_{7/2}) \rightarrow \frac{9}{2}^+(g_{7/2})$	$E2$	101
840.2	1102.3	$\rightarrow \frac{11}{2}^+(g_{7/2})$		101
	418.5	$\frac{7}{2}^+(d_{5/2}) \rightarrow \frac{7}{2}^+(g_{7/2})$		97
815.3	840.2	$\rightarrow \frac{5}{2}^+(d_{5/2})$	1.4 ± 0.3	97
	551.5 ^c	$\frac{7}{2}^+(d_{5/2}) \rightarrow \frac{7}{2}^+(g_{7/2})$		99
588.0	815.3	$\rightarrow \frac{5}{2}^+(d_{5/2})$	1.4 ± 0.4	99
	327.2	$\frac{7}{2}^+(d_{5/2}) \rightarrow \frac{7}{2}^+(g_{7/2})$	$M1$	101
879.1	588.0	$\rightarrow \frac{5}{2}^+(d_{5/2})$	0.7 ± 0.3	101
	457.4	$\frac{9}{2}^+(d_{5/2}) \rightarrow \frac{7}{2}^+(g_{7/2})$	1.5 ± 0.5	97
832.5	879.1	$\rightarrow \frac{5}{2}^+(d_{5/2})$	$E2$	97
	568.7	$\frac{9}{2}^+(d_{5/2}) \rightarrow \frac{7}{2}^+(g_{7/2})$	-1.1 ± 0.5	99
667.4	832.5	$\rightarrow \frac{5}{2}^+(d_{5/2})$	$E2$	99
	406.6	$\frac{9}{2}^+(d_{5/2}) \rightarrow \frac{7}{2}^+(g_{7/2})$	$M1$	101
1619.9	667.4	$\rightarrow \frac{5}{2}^+(d_{5/2})$	$E2$	101
	NF ^b	$\frac{11}{2}^+(d_{5/2}) \rightarrow \frac{11}{2}^+(g_{7/2})$		97

TABLE II. (Continued).

E_x (keV)	E_γ (keV)	$J_i^\pi \rightarrow J_f^\pi$	δ	Isotope ^a
	740.8	$\rightarrow \frac{9}{2}^+(d_{5/2})$	1.7 ± 0.2	97
	779.7	$\rightarrow \frac{7}{2}^+(d_{5/2})$	$E2$	97
	1198.2	$\rightarrow \frac{7}{2}^+(g_{7/2})$	$E2$	97
1468.5	398.6 ^c	$\frac{11}{2}^+(d_{5/2}) \rightarrow \frac{11}{2}^+(g_{7/2})$		99
	636.0	$\rightarrow \frac{9}{2}^+(d_{5/2})$	$0.7^{+0.8}_{-0.6}$	99
	653.2 ^c	$\rightarrow \frac{7}{2}^+(d_{5/2})$	$E2$	99
	1204.7	$\rightarrow \frac{7}{2}^+(g_{7/2})$	$E2$	99
1265.5	327.0	$\frac{11}{2}^+(d_{5/2}) \rightarrow \frac{11}{2}^+(g_{7/2})$		101
	598.1	$\rightarrow \frac{9}{2}^+(d_{5/2})$	0.5 ± 0.2	101
	677.5	$\rightarrow \frac{7}{2}^+(d_{5/2})$	$E2$	101
	1004.7	$\rightarrow \frac{7}{2}^+(g_{7/2})$	$E2$	101
1826.1	NF ^b	$\frac{13}{2}^+(d_{5/2}) \rightarrow \frac{11}{2}^+(d_{5/2})$		97
	NF ^b	$\rightarrow \frac{9}{2}^+(g_{7/2})$		97
	NF ^b	$\rightarrow \frac{11}{2}^+(g_{7/2})$		97
	947.0	$\rightarrow \frac{9}{2}^+(d_{5/2})$	$E2$	97
1649.5	NF ^b	$\frac{13}{2}^+(d_{5/2}) \rightarrow \frac{11}{2}^+(d_{5/2})$		99
	NF ^b	$\rightarrow \frac{9}{2}^+(g_{7/2})$		99
	579.7	$\rightarrow \frac{11}{2}^+(g_{7/2})$	$0.8^{+0.3}_{-1.0}$	99
	817.0	$\rightarrow \frac{9}{2}^+(d_{5/2})$	$E2$	99
1403.8	138.3	$\frac{13}{2}^+(d_{5/2}) \rightarrow \frac{11}{2}^+(d_{5/2})$		101
	NF ^b	$\rightarrow \frac{9}{2}^+(g_{7/2})$		101
	465.0	$\rightarrow \frac{11}{2}^+(g_{7/2})$	$M1$	101
	736.4	$\rightarrow \frac{9}{2}^+(d_{5/2})$	$E2$	101

^aOnly the levels up to $\frac{13}{2}^+$ and belonging to the supposed $g_{7/2}$ and $d_{5/2}$ bands have been considered in this table. The data have been taken from Ref. 6 (⁹⁷Ru), Refs. 1, 21, 22 (¹⁰¹Pd), and this work (⁹⁹Pd).

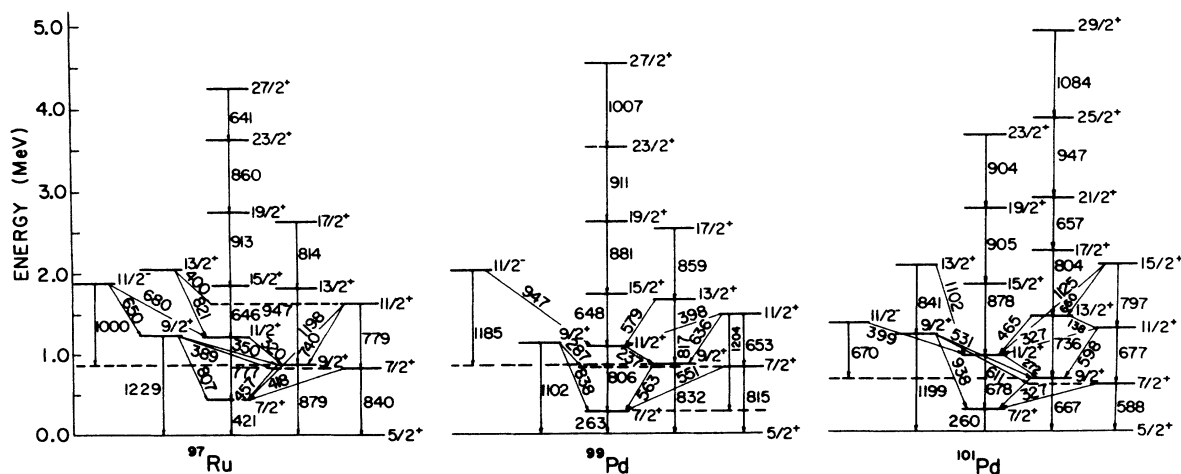
^bNot found (NF).

^cDoublet.

more strongly populated with decreasing neutron number to become the main band sequence in ⁹⁹Pd. On the other hand, a $\Delta J=1$ band on the $d_{5/2}$ ground state was observed in ¹⁰⁵Pd.³ Such a band has no counterpart in the lighter Pd nuclei where $\Delta J=2$ bands built on the $d_{5/2}$

ground state are instead detected. This structure becomes the main band sequence in ¹⁰¹Pd and is also strongly excited in ⁹⁹Pd. Similar characteristics have also been unveiled in the neighboring odd-*A* Ru nuclei.⁴⁻⁶

To have a better understanding of the different, or



similar patterns existing in the isotones ^{99}Pd and ^{97}Ru ($N=53$) and between ^{99}Pd and ^{101}Pd ($N=55$), partial level schemes of these three nuclei are shown in Fig. 7 and their deexcitation features are summarized in Table II. With the exception of the absence of the unfavored $\frac{13}{2}^+$ state in the $g_{7/2}$ band (^{99}Pd) and the energy break in the $\frac{15}{2}^+ \rightarrow \frac{11}{2}^+$ transition of the same band (^{99}Pd), the level sequence and the decay characteristics of both bands in ^{99}Pd and ^{101}Pd are very similar. For instance, the unfavored states in the $d_{5/2}$ bands have been found at lower energy than the corresponding "favored" states, whereas the opposite is true in the $g_{7/2}$ bands. Furthermore, several transitions connect the two main positive-parity bands in both nuclei, showing that some mixture of the $g_{7/2}$ and $d_{5/2}$ single-particle configurations exists. This mixture, however, is stronger in ^{99}Pd than in ^{101}Pd since considering in more detail these branchings, it is immediately clear that the interband transitions are weak in ^{101}Pd and their $E2/M1$ mixing ratios are small, whereas the same transitions are strong in ^{99}Pd and their $E2/M1$ mixing ratios become large. On the other hand, the intraband transitions are strong in both nuclei and their $E2/M1$ mixing ratios are large as well. The above

features have been well explained for ^{101}Pd (Refs. 7 and 20) by a rotational model with a Coriolis coupling at intermediate deformation, and the same model may be applicable also to ^{99}Pd . However, a larger mixing of the $g_{7/2}$ and $d_{5/2}$ single particle configurations should be considered in this nucleus.

Very similar patterns exist also in the ^{97}Ru and ^{99}Pd isotones as can be seen by an inspection of the data presented in Fig. 7 and Table II. Actually the one to one level correspondence in these two nuclei below the excitation energy of 2 MeV is remarkable (see this work and Ref. 6), and seems to show that they belong to a class of nuclei which display similar collective and shell model properties.

Finally, another significant characteristic of ^{99}Pd as well as of ^{97}Ru is the high density of their low-lying levels compared to that existing in the other isotones ($N=53$) ^{93}Zr and ^{95}Mo .¹⁸ Clearly the increasing proton number plays an important role in ^{97}Ru and ^{99}Pd making these nuclei more susceptible to collective motions and thus more similar in their features to the richer neutron nuclei of this transitional region.

¹P. C. Simms, G. J. Smith, F. A. Rickey, J. A. Grau, J. R. Tesmer, and R. M. Steffen, *Phys. Rev. C* **9**, 684 (1974).
²J. A. Grau, F. A. Rickey, G. J. Smith, P. C. Simms, and J. R. Tesmer, *Nucl. Phys. A* **229**, 346 (1974).
³F. A. Rickey, J. A. Grau, L. E. Samuelson, and P. C. Simms, *Phys. Rev. C* **15**, 1530 (1977).
⁴G. Kajrys, R. Lecomte, S. Landsberger, and S. Monaro, *Phys. Rev. C* **28**, 1504 (1983).
⁵C. S. Whisnant, R. H. Castain, F. A. Rickey, and P. C. Simms, *Phys. Rev. Lett.* **50**, 724 (1983).
⁶G. Kajrys, J. Dubuc, P. Larivière, S. Pilotte, W. Del Bianco, and S. Monaro, *Phys. Rev. C* **34**, 1629 (1986).
⁷Hasting A. Smith, Jr., and F. A. Rickey, *Phys. Rev. C* **14**, 1946 (1976).
⁸Rakesh Popli, J. A. Grau, S. I. Popik, L. E. Samuelson, F. A. Rickey, and P. C. Simms, *Phys. Rev. C* **20**, 1350 (1979).
⁹P. Chowdhury, B. A. Brown, U. Garg, R. D. McKeown, T. P. Sjoreen, and D. B. Fossan, *Phys. Rev. C* **32**, 1238 (1985).
¹⁰J. S. Kim, Y. K. Lee, K. A. Hardy, P. C. Simms, J. A. Grau, G. J. Smith, and F. A. Rickey, *Phys. Rev. C* **12**, 499 (1975).
¹¹W. F. Piel, Jr., and G. Scharff-Goldhaber, *Phys. Rev. C* **15**, 287 (1977).

¹²A. H. Lumpkin, L. H. Harwood, L. A. Parks, and J. D. Fox, *Phys. Rev. C* **17**, 376 (1978).
¹³G. Kajrys, M. Irshad, S. Landsberger, R. Lecomte, P. Paradis, and S. Monaro, *Phys. Rev. C* **26**, 138 (1982).
¹⁴M. Huyse, K. Cornelis, G. Lhersonneau, J. Verplancke, W. B. Walters, K. Heyde, P. Van Isacker, M. Waroquier, G. Wenes, and H. Vincx, *Nucl. Phys. A* **352**, 247 (1981).
¹⁵J. T. Routti and S. G. Prussin, *Nucl. Instrum. Methods* **72**, 125 (1969).
¹⁶P. Taras and B. Haas, *Nucl. Instrum. Methods* **123**, 73 (1975).
¹⁷H. J. Rose and D. M. Brink, *Rev. Mod. Phys.* **39**, 306 (1967).
¹⁸*Table of Isotopes*, 7th ed., edited by C. M. Lederer and V. S. Shirley (Wiley, New York, 1978), p. 429.
¹⁹S. Landsberger, R. Lecomte, P. Paradis, and S. Monaro, *Phys. Rev. C* **21**, 588 (1980).
²⁰P. Fettweis, P. del Marmol, M. Degreef, P. Duhamel, and J. Vanhorenbeeck, *Z. Phys.* **305**, 57 (1982).
²¹Rakesh Popli, F. A. Rickey, and P. C. Simms, *Phys. Rev. C* **22**, 1121 (1980).
²²P. Larivière, M. Sc. thesis Université de Montréal, 1987 (unpublished).